Annu. Rev. Phys. Chem. 1991. 42: 731–68

STRATOSPHERIC OZONE DEPLETION

F. Sherwood Rowland

Department of Chemistry, University of California, Irvine, California 92717

KEY WORDS: chlorofluorocarbon, Antarctic, chlorine chain reactions, nitrogen oxide chain reactions, anthropogenic

INTRODUCTION

Although atmospheric ozone has a recorded history dating back to the ancient Greeks, scientific interest in stratospheric ozone only began in the last century, when Hartley (1) recognized that the 293 nm cut-off in solar ultraviolet (UV) radiation at the Earth's surface corresponded very closely with the UV absorption spectrum of O_3. When his further experiments at mountain altitudes (2) displayed an unchanged solar UV cut-off, the groundwork was laid for our present understanding that about 90% of the atmospheric ozone lies in the stratosphere. Knowledge of the Earth's ozone distribution was outlined in the 1920s and 1930s by a series of experimenters, especially G. M. B. Dobson, who adapted the existing UV spectrometers into an instrument suitable for daily measurements in remote locations by trained technicians (3). With such instruments transported to various remote sites, the ozone levels in the temperate zones were demonstrated to be higher than in the tropics. Although the tropical latitudes have approximately 260 milliatmosphere centimeters of O_3 (or Dobson Units) year-round, temperate zone stations exhibit strong seasonal variations with a maximum peaking in March/April and a minimum in October/November in the northern hemisphere, and the reverse in the southern hemisphere (Figure 1) (4).

The logical source for this ozone was the solar UV photolysis of molecular oxygen by Equation 1, followed by combination with another O_2 molecule in Equation 2, but, if so,

0066–426X/91/1101–0731$02.00

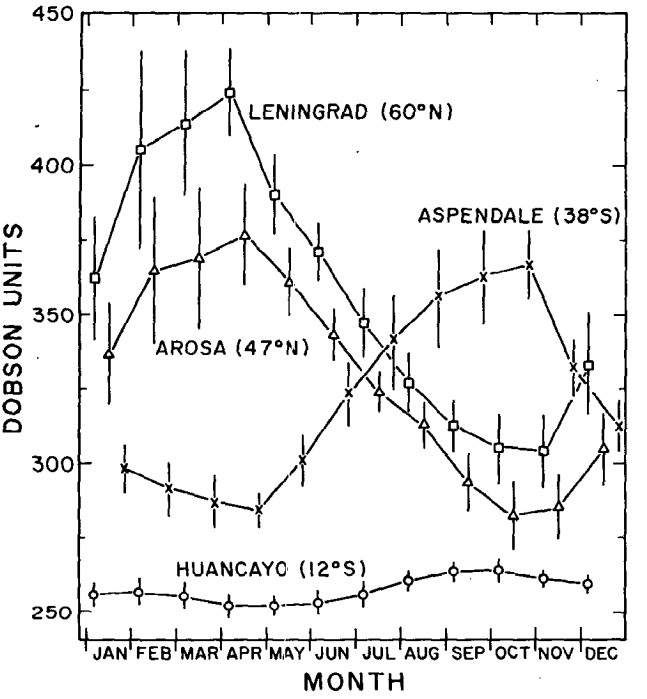

Figure 1 Monthly average ozone concentrations for four ground stations with interannual standard deviations. (□ = Leningrad, U.S.S.R.; △ = Arosa, Switzerland; × = Aspendale, Australia; ○ = Huancayo, Peru.)

$$O_2 + UV(\lambda < 242\,nm) \rightarrow O + O \qquad 1.$$

$$O + O_2 + M \rightarrow O_3 + M \qquad 2.$$

why was the concentration of stratospheric ozone not highest in the tropics, where the solar radiation was most intense?

In 1930, Chapman (5) provided a qualitative and approximately quantitative explanation for this unexpected latitudinal and seasonal distribution of ozone. He added Equations 3 and 4 to the sequence, including the crucial step that the conversion of O_3 back to

$$O_3 + UV \rightarrow O + O_2 \qquad 3.$$

$$O + O_3 \rightarrow O_2 + O_2 \qquad 4.$$

O_2 in Equation 4 is also initiated by solar UV radiation through its release of atomic O in Equations 1 and 3. With both a source and sink for ozone located predominantly in the upper stratosphere of the tropics, the

amounts of ozone found elsewhere depend upon a complex interplay between the molecular transformations of chemistry and meteorological transport to other altitudes and latitudes. Investigations in the 1930s established that the maximum concentrations of ozone lie in the lower stratosphere between 15–25 km, which further emphasized the role of atmospheric transport in determining the distribution of ozone. Within the quantitative limitations imposed by laboratory measurements of the reaction rates for Equations 1–4 and especially by the absence of detailed solar UV spectra beyond the atmosphere, these four oxygen, or "Chapman," reactions provided a satisfactory explanation for the origin and distribution of atmospheric ozone for more than three decades.

The modern era of stratospheric ozone studies began in the 1960s, with proposals that the detailed ozone source/sink calculations were not in balance: Less ozone was actually present than would be expected from the Chapman reactions alone, and some additional sink for ozone must exist (4). This gap has now been closed with the progressive inclusion of a series of free radical catalytic chains, of which the most important are the HO_x, NO_x (6, 7), and ClO_x (8, 9) sequences, as shown in Equations 5–8 for the latter two. Each of these chains sums to the equivalent of the direct Equation 4. Most numerical

$$NO + O_3 \rightarrow NO_2 + O_2 \qquad 5.$$

$$NO_2 + O \rightarrow NO + O_2 \qquad 6.$$

SUM: $O + O_3 \rightarrow O_2 + O_2$

$$Cl + O_3 \rightarrow ClO + O_2 \qquad 7.$$

$$ClO + O \rightarrow Cl + O_2 \qquad 8.$$

descriptions of ozone production and loss are described in terms of traces of "odd oxygen" (i.e. O plus O_3, in contrast to the abundant "even oxygen," O_2), because the photochemical destruction of O_3 in Equation 3 does not result in permanent ozone removal if the O atom so released immediately reforms O_3 by Equation 2. In the odd oxygen calculus, Equations 2 and 3 have values of zero, with +2 for Equation 1, −2 for Equation 4, and −1 each for Equations 5–8. The major share of atmospheric odd oxygen removal is carried by the free radical chains (4).

The inclusion of chain reactions in the ozone balance requires description of the sources of the chain carriers, the possibility for temporary or permanent interruption of the chains by the formation of reservoir compounds (e.g. $ClO + NO_2 \rightarrow ClONO_2$, chlorine nitrate), and the eventual permanent sinks for the chain carriers. Furthermore, the realization

over the past two decades that some of the sources for the chain carriers have been substantially augmented by human activities has raised major concerns about the possibilities of significant stratospheric ozone depletion in the coming half century (6–9).

PRECURSORS FOR STRATOSPHERIC CHAIN REACTIONS

Two major methods exist for introducing chain carriers, such as HO, NO, or Cl, into the stratosphere: direct physical deposition and release into the troposphere of a sufficiently inert chemical compound, of which a significant fraction survives to drift randomly into the much more intense solar UV radiation of the midstratosphere. The increased photochemical reactivity of 30 km or higher is largely the consequence of being at altitudes above most of the O_2 and O_3 that absorb UV by Equations 1 and 3.

Direct physical formation of NO in the stratosphere can be accomplished simply by heating N_2 and O_2 together, as with air drawn into the fireball of an atmospheric nuclear weapons test (10, 10a) or through the engine of a high-flying aircraft (11). At the beginning of the twentieth century, sources already existed in the natural atmosphere that served as the inert precursors for delivery of H, NO and Cl to the stratosphere. Two compounds, H_2O and CH_4, serve as the primary carriers for introducing H into the stratosphere. Entrance is essentially limited meteorologically to large air masses that rise in tropic latitudes and pass through the cold trap of the tropical tropopause at temperatures around $-78°C$, thereby limiting the initial stratospheric water vapor content to about 3 parts per million by volume (ppmv). These rising air masses also transport trace gaseous molecules without regard to their molecular weights—the gravitational separation of atmospheric components by molecular diffusion is overwhelmed by large convective motions to altitudes far above the top of the stratosphere.

Among the molecules transported through the tropical tropopause with H_2O are CH_4, N_2O, and CH_3Cl. Both CH_4 and CH_3Cl have sinks in the troposphere through reaction with HO radical, as in Equations 9 and 10, but have atmospheric lifetimes long enough

$$HO + CH_4 \rightarrow H_2O + CH_3 \qquad 9.$$

$$HO + CH_3Cl \rightarrow H_2O + CH_2Cl \qquad 10.$$

[about 10 years and 1.5 years, respectively (12, 13)], that appreciable concentrations exist in the upper troposphere in tropic latitudes. Once in

the stratosphere, CH_3Cl is still susceptible to HO attack and eventually releases both H and Cl.

The measured tropospheric concentrations of CH_3Cl are approximately 600 parts per trillion by volume (pptv) and have shown no discernible trend during 15 years of accurate assay (4, 13). The currently available data suggest that the stratospheric mixing ratio of Cl summed over all chemical forms a century ago was not much larger than that furnished by CH_3Cl alone (i.e. about 600 pptv). Measurement of the CH_3Cl concentrations in glacial ice cores has not yet been accomplished, but when completed, can provide information about any variations in the stratospheric Cl burden over the past 160,000 years or longer.

Because mixing in the stratosphere is not affected by changes in chemical form, the mixing ratio (i.e. mole fraction) of Cl from CH_3Cl will be essentially constant throughout the atmosphere from the surface to 50 km and above, as shown in Figure 2. Although the chemical form of the Cl atom is initially CH_3Cl, smaller and smaller fractions survive unchanged to higher altitudes (14), and a larger and larger fraction is distributed among the available forms of inorganic chlorine—chiefly Cl, ClO, HCl, $ClONO_2$, and HOCl. Redistribution of Cl among these compounds is

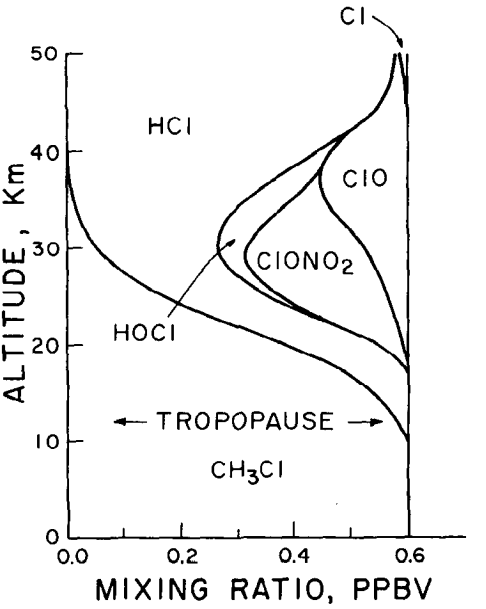

Figure 2 Chemical distribution versus altitude for Cl from surface emissions of methyl chloride.

controlled by the various chemical and photochemical reactions that affect these molecules at each altitude (15). The lower temperatures of the stratosphere, as low as −67°C at 20 km in temperate latitudes and −90°C in polar latitudes, control the rates of the chemical reactions, whereas the intensity of solar UV radiation becomes rapidly greater at higher altitudes with less and less shielding by O_2 and O_3. Both HOCl and $ClONO_2$ have significant absorption cross-sections at wavelengths beyond 293 nm (15) and are, therefore, subject to solar photodecomposition throughout the atmosphere, albeit more intensively at higher altitudes.

The total amount of H in the stratosphere is essentially the sum of the amounts delivered there as H_2O and CH_4. The mixing ratio of CH_4 at the 50 km level is only about one eighth the value at the tropopause, with the remaining seven-eighths already oxidized and converted to H_2O. Satellite measurements of the concentrations of both CH_4 and H_2O have confirmed that the sum of the H present is nearly constant for all stratospheric latitudes and altitudes (16, 16a) at 12–13 ppmv (e.g. 3 ppmv $H_2O \times 2$ H atoms/molecule plus 1.5 ppmv $CH_4 \times 4$ atoms/molecule). Molecular H_2O is much more stable in the stratosphere than either CH_4 or CH_3Cl, with the consequence that only a very minor fraction of the H is present in the free radical forms *H*, *HO*, HO_2, or more reactive compounds, such as HNO_3, HOCl, or H_2O_2.

Unlike CH_3Cl, the measurements of the past decade have clearly shown that the tropospheric concentrations of methane have been increasing (Figure 3) on a global scale, from about 1.52 ppmv in 1978 to 1.71 ppmv in 1990 (17, 17a). A corollary consequence is that the amounts of H carried into the stratosphere have probably been steadily increasing: If H_2O content remained constant at an average of about 3 ppmv, then the observed CH_4 change would raise total H from 12.1 ppmv in 1978 to 12.8 ppmv in 1990 (17, 17a). Measurements of methane in glacial ice cores have established that the atmospheric CH_4 level was about 0.7 ppmv in 1800 (18, 18a), and as low as 0.3 ppmv during the ice ages 20,000–160,000 years ago (19). Thus the total delivery of H to the stratosphere has probably increased 50% to its present level from about 9 ppmv H two centuries ago. This conclusion depends implicitly on the plausible assumption, untestable in the absence of any pertinent data, that the average temperature of the tropical tropopause—and thereby control of the freeze-drying of air entering the stratosphere—has remained unchanged during that period.

The extent to which this 100+% increase in CH_4 concentrations is anthropogenic in origin is quantitatively uncertain, but all of the major biological emission sources for CH_4 (cattle, rice paddies, swamps) and the nonbiological sources associated with fossil fuels have been perturbed by mankind during the past two centuries (20). An increase in total H in the

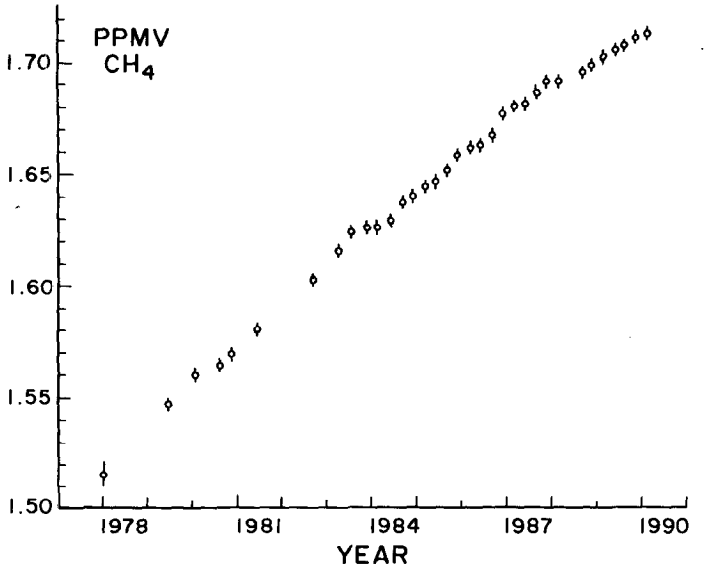

Figure 3 Global average concentrations of atmospheric methane, 1978–1990.

stratosphere then impacts directly on the ambient ozone concentrations through altered levels of HO and HO_2, and indirectly from the likely increase in both frequency and total volume of clouds in the stratosphere. The role of polar stratospheric clouds (PSCs) in stratospheric ozone depletion is particularly important, as discussed later.

Direct emissions of the NO_x free radicals into the troposphere, or formation there by the action of lightning, have little effect on the stratosphere, because rainout can remove oxygen-bonded N from the atmosphere while in the form of nitric acid or in other water-soluble chemical forms (e.g. peroxyacetyl nitrate). The major source of NO and NO_2 in the stratosphere is N_2O emitted at the surface. Current knowledge indicates that N_2O has no significant tropospheric sink and an average lifetime in the atmosphere of 150 years (13, 14). Its most important sources are microbiological activity in the soil and the oceans, resulting from side pathways during the nitrification to N_2 of NH_3 or the denitrification of NO_3^-. In the stratosphere, the molecule can be destroyed by either direct photolysis, as in Equation 11, or reaction with $O(^1D)$ atoms in Equation 12. Approximately 90% of N_2O removal occurs by photolysis, so

$$N_2O + UV \rightarrow N_2 + O \qquad 11.$$

$$N_2O + O(^1D) \rightarrow NO + NO \qquad 12.$$

that most N atoms delivered to the stratosphere as N_2O are converted directly into inert N_2. However, the lesser pathway for N_2O by Equation 12 is the major source of stratospheric NO_x. The chief source for $O(^1D)$ in both the troposphere and the stratosphere is Equation 3′ when initiated by UV radiation with wavelengths shorter than 314 nm. The reaction of $O(^1D)$ with H_2O vapor in the troposphere by Equation 13 is the ultimate source for HO, the primary oxidant of trace compounds introduced near the Earth's surface.

$$O_3 + UV \rightarrow O(^1D) + O_2 \qquad 3'.$$

$$O(^1D) + H_2O \rightarrow HO + HO. \qquad 13.$$

ANTHROPOGENIC INCREASES IN PRECURSOR CONCENTRATIONS

The natural transport to the stratosphere of H_2O, CH_4, N_2O, and CH_3Cl established a complex chemistry that regulated the concentrations of ozone and a substantial number of temporary reservoir compounds formed by the chain-terminating combination reactions of the various free radical chain carriers: HNO_3, HO_2NO_2, N_2O_5, H_2O_2, HCl, $ClONO_2$, HOCl. As the concentrations of the precursors increase in the troposphere, those of the free radicals in the stratosphere respond quickly to these alterations in their support base. The global average concentration of N_2O has been increasing recently at a rate of 0.2% per year (4, 21) to a 1990 value of about 308 parts per billion by volume (ppbv). Several potential causes for this increase have been postulated, including combustion of fossil fuel and the increased use of nitrogenous fertilizers in agriculture. However, quantitative evaluation of such sources has remained elusive, at least in part because measurement of N_2O has been complicated through its formation as a contaminant by surface reactions among components trapped in air sampling canisters (22, 23).

During the last 30 years, the most striking increases in stratospheric free radical concentrations are those associated with the ClO_x chains through the widespread global usage of volatile synthetic organochlorine compounds. The most important of these, in terms of quantitative contributions to stratospheric concentrations of Cl and ClO, have been CH_3CCl_3, CCl_4, and the chlorofluorocarbons (CFCs), of which CCl_2F_2 (CFC-12), CCl_3F (CFC-11), and CCl_2FCClF_2 (CFC-113) are the most abundant (24). None of these anthropogenic perhalocarbon compounds have an important tropospheric sink, with the consequence that their atmospheric lifetimes are controlled by UV photochemistry in the stratosphere. Because the UV photochemical cross-sections of CCl_4 and CFCs

are fully screened by ozone in the troposphere and lower stratosphere, photodecomposition by solar UV, as in Equation 14 for CCl_3F, is negligibly slow below about 20 km and then rises rapidly higher in the stratosphere. Although the photolysis rate continues to increase to the top of the atmosphere, the actual photolysis reaches its peak at altitudes around 30 km. Atomic Cl released in Equation 14 in turn induces the ClO_x chain reaction of Equations 7 and 8. The interconnection between CFCs and stratospheric

$$CCl_3F + UV\,(\lambda < 230\,nm) \rightarrow Cl + CCl_2F \qquad 14.$$

ozone is, therefore, very direct—photolysis of CFCs begins only at altitudes for which they are no longer protected by ozone absorption of UV radiation. Although the ClO_x chain can be temporarily interrupted by the formation of a reservoir compound, such as $ClONO_2$ or HCl, photolysis or HO attack releases Cl, and the ClO_x chain begins anew until the Cl atom has diffused back into the troposphere. The average Cl atom removes about 10^5 ozone molecules before final termination by rainout of HCl.

The atmospheric lifetimes of CFC-11 and CFC-12 were initially postulated to lie in the 40–80 year and 80–150 year ranges, respectively, through model atmospheric calculations based on their known photochemistry (9). Close comparisons of the amounts in the atmosphere versus the totals already emitted have led to best estimates of 75 years and 110 years, respectively, for CFC-11 and CFC-12 (25). The atmospheric lifetime of CFC-113 is slightly shorter than for CFC-12, and that of CCl_4 must also be 50 years or more. The residual radicals, such as Cl_2F from Equation 14, react immediately with O_2, thus releasing a second Cl atom and leaving an oxygenated residue, CClFO in this instance. Although such compounds are expected in the stratosphere (9a, 26), and CCl_2O has also been observed in the troposphere (27), most are further dissociated, releasing both Cl and F. The eventual fate of F is the formation of HF, whose concentration has been shown from infrared spectra to have increased fourfold since 1978 (4, 28). Atomic F and the radical FO can remove ozone by an FO_x chain analogous to the ClO_x chain of Equations 7 and 8, but the chain is quickly terminated by the formation of HF, which is itself chemically inert, thus preventing further ozone loss.

The yearly world release to the atmosphere of CFCs exceeds 1 million tons per year, essentially all of which eventually decomposes in the stratosphere (24). The total world production of volatile chlorinated organic molecules is many times larger than that of the CFCs, but two factors reduce or eliminate the stratospheric ozone threat from these high-volume chlorocarbons. Many are industrial precursors of nonvolatile compounds whose Cl atoms never enter the atmosphere, as with CH_2ClCH_2Cl or

CH_2=CHCl used sequentially in the production of the plastic polyvinylchloride. Others, such as CHCl=CCl_2, are emitted to the atmosphere, but are so chemically reactive that they survive for only a few weeks, with the Cl atoms rapidly converted to water-soluble compounds, such as HCl, which are removed by rain. Similar fates make tropospheric inputs of HCl and salty oceanic sea spray of negligible stratospheric importance.

In contrast to the CFCs and CCl_4, the atmospheric lifetime of CH_3CCl_3 is controlled through reaction with HO in the troposphere by Equation 15. In this case, with

$$HO + CH_3CCl_3 \rightarrow H_2O + CH_2CCl_3 \qquad 15.$$

reasonably accurate global estimates available of total manufacture and release, comparisons of atmospheric concentrations with cumulative emissions have shown that only about half of the CH_3CCl_3 emitted to the atmosphere is still there, which corresponds to an atmospheric lifetime of about six or seven years, with an accuracy of about $\pm 20\%$ (12, 29, 30).

This CH_3CCl_3 calculation plays a central role in considerations of the atmospheric lifetimes of other hydrogen-containing molecules, because measurements of the tropospheric concentrations of HO radicals have proven to be an exceedingly elusive target (31). Only a few actual measurements of HO concentrations have succeeded, no portable instruments have yet been successfully applied, and direct global assays of HO are therefore totally absent (32). In these circumstances, an indirect measurement of global HO strength is indispensable, and the atmospheric lifetime of CH_3CCl_3 coupled with the measured laboratory reaction rate for Equation 15 can be used to indicate a 24-hour global average concentration of about 6×10^5 HO radicals/cm^3.The lifetimes of other C–H containing molecules can then be inferred from the inverse ratio of the measured laboratory reaction rates with HO radicals. This procedure has been extensively applied for estimates of the atmospheric lifetimes for various molecules already known to be in the atmosphere and for evaluation of molecules newly proposed for widespread release as substitutes for CFCs, as shown in Table 1 (12, 13, 33, 34). The substitutes are now usually designated as HCFCs (e.g. $CHCl_2CF_3$ as HCFC-123) or HFCs (e.g. CH_2FCF_3 as HFC-134A) to distinguish them from the CFCs, as the latter come under various regulatory edicts.

The capability for stratospheric ozone depletion by a particular organochlorine compound is basically a consequence of its ability to deliver chlorine to the stratosphere and is primarily a function of its number of chlorine atoms and atmospheric lifetime, but the details of its stratospheric reactivity are also important. The more Cl atoms per molecule, the more

Table 1 Hydroxyl reaction rates, atmospheric lifetimes, and ozone depletion potentials for various hydrocarbons and halocarbons

Molecule	k_{280} cm^3 $molecule^{-1}$ sec^{-1}	Lifetime	Ozone depletion potential
CH_3CCl_3	8.2×10^{-15}	(6.5 yrs.)	0.11
CH_4	5.6×10^{-15}	10 yrs.	0
C_2H_6	2.2×10^{-13}	2 mos.	0
C_3H_8	9.7×10^{-13}	3 wks.	0
CH_3Cl	3.5×10^{-14}	1.5 yrs.	—
$CHCl_3$	8.3×10^{-14}	8 mos.	—
$CHClF_2$	3.4×10^{-15}	16 yrs. HCFC-22	0.053
$CHCl_2CF_3$	2.7×10^{-14}	2.0 yrs. HCFC-123	0.016
$CHClFCF_3$	7.6×10^{-15}	7 yrs. HCFC-124	0.019
$CH_2ClCClF_2$	1.1×10^{-14}	1.3 yrs. HCFC-132	~0.01
CH_2FCF_3	6.4×10^{-15}	8 yrs. HFC-134A	0
CCl_2FCH_3	5.5×10^{-15}	10 yrs. HCFC-141B	0.08
$CClF_2CH_3$	2.4×10^{-15}	22 yrs. HCFC-142B	0.06
CH_3CHF_2	2.6×10^{-14}	2.1 yrs. HCFC-152A	0
CCl_3F	0	75 yrs. CFC-11	(1.0)
Ozone Depletion Potentials for:	CCl_2F_2	1.0	
	CCl_4	1.1	
	CCl_2FCClF_2	0.82	

delivered to the stratosphere; the shorter the lifetime, the more molecules deposit Cl in the troposphere, and, therefore, do not deplete ozone in the stratosphere. The ozone depletion potentials (ODPs) of the substitute HCFCs, which are also given in Table 1 (33, 34), represent the relative amount of ozone depletion calculated in atmospheric models in comparison to the losses from an equivalent tonnage of CFC-11 set as 1.0. The CFC-11 calculations demonstrate ozone depletion extending well beyond 100 years into the future, whereas that from HCFCs tends to be concentrated in the very near future because of their shorter lifetimes. For this reason, calculations have also been conducted to determine transient ODPs, which average the future ozone losses from HCFC and CFC-11 over the next 25–50 years, and these are arguably more appropriate for regulatory considerations (34). Questions have also been raised about the appropriateness of the existing atmospheric model calculations of ODP values (35), because substantial fractions of ozone losses in the real atmosphere occur in polar vortices under the influence of heterogeneous chemical reactions, whereas the models used for ODP calculations have as yet only considered homogeneous gas phase reactions.

The concentrations of various organochlorine compounds have been

measured in the atmosphere since the mid-1970s, with sufficient information now available to permit extrapolation backward in time to the pre-CFC era and forward beyond 1990 in anticipation of various proposed scenarios for future emissions, as shown in Figure 4 (24). Typical gas chromatographic measurements of halocarbon concentrations in one remote and two urban locations are shown in Figure 5. Seven major organochlorine compounds are identified in the air sample from Tokyo, together with 11 additional compounds present in minor yield. (The instrumental sensitivities are greatest for CFC-11, CCl_4, and CH_3CCl_3 and are an order of magnitude less for CFC-12 and CFC-113.) Six of the seven major compounds were also found in Santa Clara, California, and outside Barrow, Alaska. The concentrations in Barrow are, however, much smaller, and most of the minor peaks in the urban locations are essentially absent in northern Alaska, which is distant from the largely urban sources. Measurements in remote locations over all latitudes furnish the basis for a global assay. Figure 6 illustrates a background latitudinal distribution of CCl_3F (36). Approximately 95% of chlorocarbon release occurs in the northern hemisphere, but transport time of about one year between the

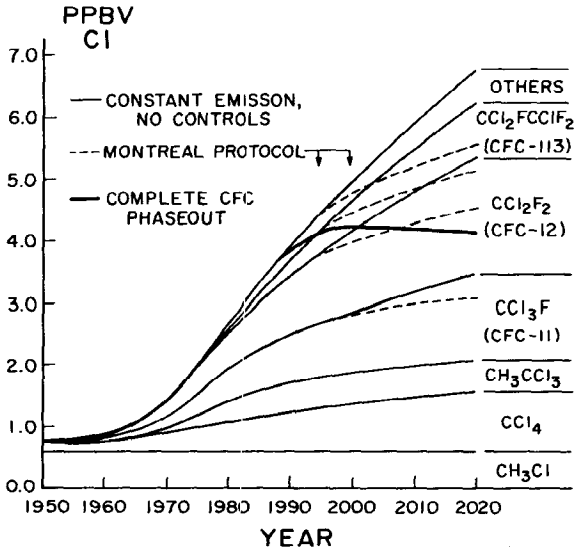

Figure 4 Tropospheric organochlorine concentrations from 1950 to 2020. Data through 1990 based on measurements from 1975–1990. Calculated future concentrations on several bases: yearly emissions remain constant at 1986 levels (*solid line*); yearly emissions of CFCs reduced in accord with Montreal Protocol of 1987 (20% decrease in 1994, additional 30% decrease in 1999) (*broken line*); linear reduction in emissions of CFCs over decade of 1990s, with zero CFC emissions in 2000 and thereafter (*bold line*).

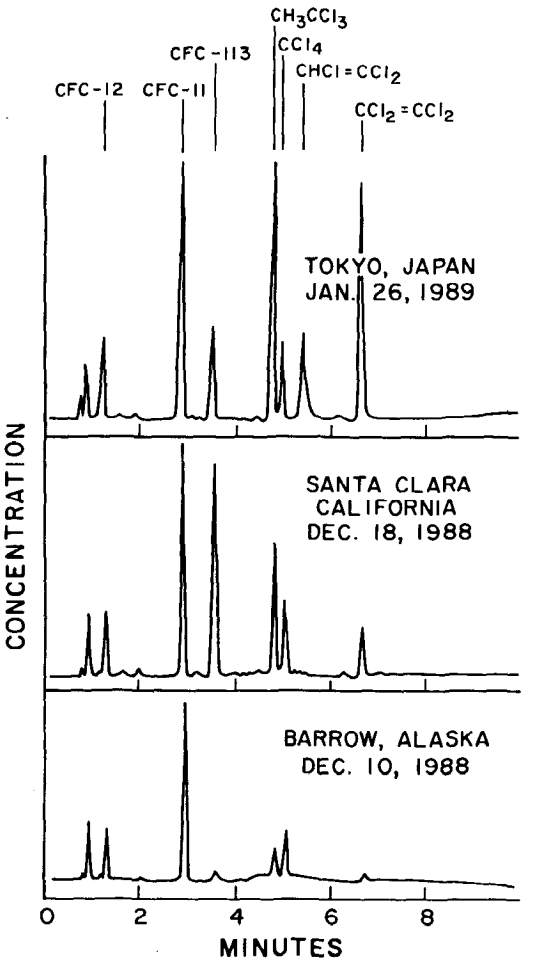

Figure 5 Halocarbon measurements by electron capture gas chromatographic analysis for three air samples: (*top*) Tokyo, Japan; (*middle*) Santa Clara, California; (*bottom*) upwind from Barrow, Alaska (71° North Latitude).

northern and southern hemispheres keeps the interhemispheric gradient small. Figure 4 shows that the total organochlorine concentration, only 0.6 ppbv in 1900 largely from CH_3Cl, has increased in the troposphere from 0.8 ppbv in 1950 to about 4.0 ppbv in 1990. The stratospheric concentration of total chlorine will follow along with a delay period of 5–10 years for trophospheric mixing and upward transfer and then photodecomposition at stratospheric altitudes.

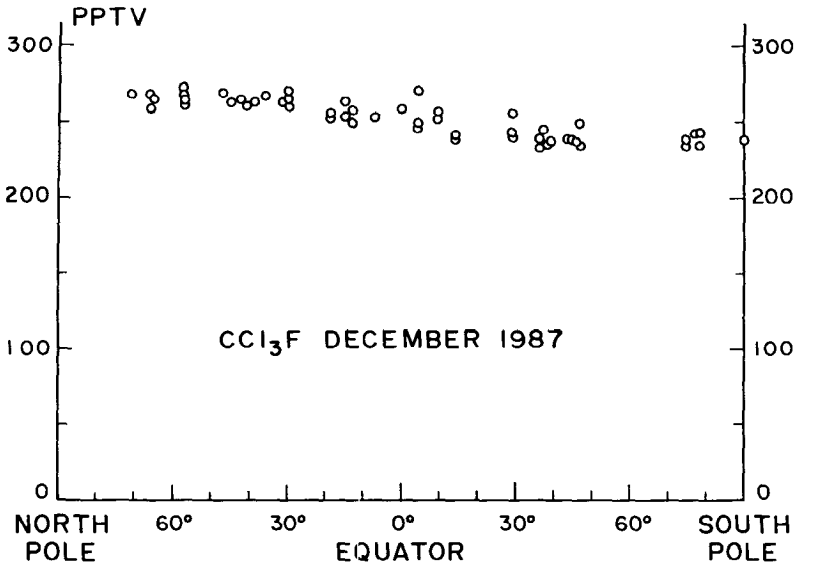

Figure 6 Latitudinal distribution of CCl_3F concentrations in remote locations.

STRATOSPHERIC SOURCES OF FREE RADICALS

The possibility of stratospheric ozone depletion through direct release of free radicals into the stratosphere was first considered in connection with the proposals in 1970 for construction of supersonic transport aircraft (SSTs), because of the partial conversion of N_2/O_2 into NO in their engines (11). The important parameter is not the supersonic speeds of the aircraft, but the flight altitudes of 17 km for the Anglo-French Concorde and 20 km for the proposed Boeing SST. Indeed, far greater quantities of air are converted into NO in the engines of automobiles, and NO_x at ground level is a major contributor to the formation of additional O_3 in photochemical smog. The chemical sequence at the surface involves the formation of carbonaceous free radicals by HO attack on hydrocarbons and other organic molecules, as in Equation 16, which is followed by oxygenation of the residual organic radical in Equation 17, reaction with NO to form NO_2 in Equation 18, and then photolysis of NO_2 in Equation 19 to release

$$HO + RH \rightarrow H_2O + R \qquad 16.$$

$$R + O_2 \rightarrow RO_2 \qquad 17.$$

$$RO_2 + NO \rightarrow RO + NO_2 \qquad 18.$$

$$NO_2 + h\nu \rightarrow NO + O \qquad 19.$$

NO again, plus an O atom that is converted to O_3 by Equation 2. The difference between this sequence and the NO_x chain in the upper stratosphere lies in the much greater frequency of the reaction of NO_2 with O in the latter—a process that removes an atom of oxygen versus photolysis, which produces an additional oxygen atom.

The competition for NO_2 between reaction with O (ozone depletion) and photolysis (ozone formation) is highly dependent on altitude and solar angle. The competition has always implied (11) the existence of a "crossover" altitude above which NO_x emissions tend to deplete ozone and below which NO_x emissions, when combined with abundant hydrocarbon emissions, produce enhanced ozone concentrations. Stratospheric model calculations of ozone changes versus altitude have proven to be quite sensitive to some of the input data, and especially to major revisions of chemical or photochemical rate constants or to the inclusion of additional chemical reactions of newly found importance (4, 14). A further complication is introduced by the interactions between different free radical chains, so that enhanced NO_x concentrations can simultaneously increase the removal of ozone by Equations 5 and 6 and reduce the removal of ozone by Equations 7 and 8 through the sequestration of ClO as $ClONO_2$.

In 1975, the calculated impact of 500 airplane fleets of the Concorde or Boeing SST aircraft was substantial ozone depletion on a global basis (11). The calculated quantitative impact of equivalent NO_x injections has varied in the ensuing 15 years, with each elaboration of the chemical basis of the atmospheric models; for a brief time around 1980, the calculations indicated that a large fleet of Concorde-type aircraft would have slightly enhanced total stratospheric ozone (4). Although the latter conclusion became frozen in place in aeronautic circles and in the Department of Transportation, not to be reexamined for almost a decade, since 1980, the atmospheric models have predicted that substantial ozone depletion would accompany such large high-altitude fleets (4). The most recent thorough reevaluation (37) has indicated losses comparable to those originally estimated in 1975. Furthermore, calculations have now been performed with two-dimensional models, with both latitude and altitude as parameters. Figure 7 illustrates the calculated ozone depletions for the Boeing fleet, and Table 2 provides the ozone losses calculated with the one-dimensional models for various improved engine efficiencies (with respect to NO_x emissions) (37). At the same time, the much larger emissions from the existing subsonic commercial aircraft fleet, with flight altitudes around 10–12 km, are calculated in the 1990 versions of

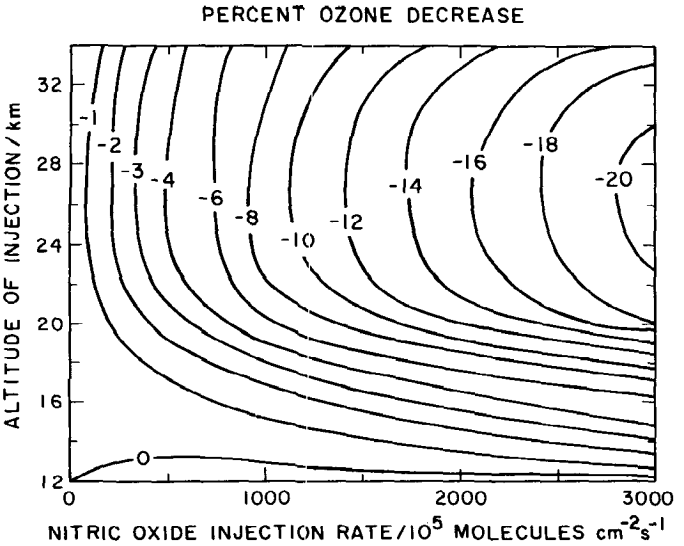

Figure 7 Altitude dependence of percentage change in total column ozone, LLNL 1-D Model. Emissions assumed for 1 km band centered at given altitude.

atmospheric models to cause a slight increase in total stratospheric ozone (4, 13).

Nuclear weapons testing in the atmosphere has long been known to be another source for the direct introduction of NO_x through air drawn into the nuclear fireball (10, 10a). Calculation of the overall effect has indicated stratospheric ozone depletion, especially during the early 1960s, when large

Table 2 Calculated change in global-averaged total ozone from the LLNL two-dimensional model, which assumes an annual fuel consumption of 7.7×10^{10} kg, with all emissions between 37°–49°N in a 3 km altitude range centered about 22.5 km altitude (relative to an atmosphere with no aircraft emissions), based on Ref. 37

Emission scenario	Emission index g of NO kg^{-1} fuel	Injection rate: MT of NO_2 yr^{-1}	Injection rate: Molecules/ 10^5 cm^{-2} s^{-1}	Change in total ozone
Current subsonic rate	40[a]	4.8	4000	−19.0%
Standard CIAP rate	15	1.8	1500	−8.6%
Future goal	5	0.6	500	−2.8%

[a] This emission index assumes current commercial subsonic aircraft technology being used in the stratosphere. The actual emission index for current aircraft at their flight altitudes in the upper troposphere are a factor of 2–3 smaller than this.

weapons were being tested by both the United States and the Soviet Union. The results from a recent recalculation, which are illustrated in Figure 8, indicate that the largest depletions in ozone should have occurred at higher latitudes in the northern hemisphere. The ozone depletion effects that would accompany an all-out exchange of nuclear weapons have been calculated to be much more severe. Under the circumstances, however, these effects are overshadowed by the direct destructive effects of nuclear explosions and by the estimated "nuclear winter" consequences of the smoke and dust thrown into the atmosphere by the explosions and subsequent conflagrations (38, 39).

An additional source for direct introduction of free radicals into the stratosphere is the firing of rocket payloads into space (8, 40), as with the Space Shuttle whose first-stage rockets contains approximately 100 tons of chlorine as ammonium perchlorate (mixed with powdered aluminum). With first-stage burnout at altitudes between 40–45 km, as much as half of this chlorine is deposited in the stratosphere, probably initially as HCl. Although the intense UV exposure of the middle and upper stratosphere ensures that essentially all forms of chlorine are quickly thrown into the appropriate chemical equilibrium involving Cl, ClO, and the various temporary reservoirs, the cumulative introduction of chlorine into the stratosphere at 50 tons per large rocket firing is small compared with the millions of tons of chlorine injected into the atmosphere through the release of organochlorine compounds.

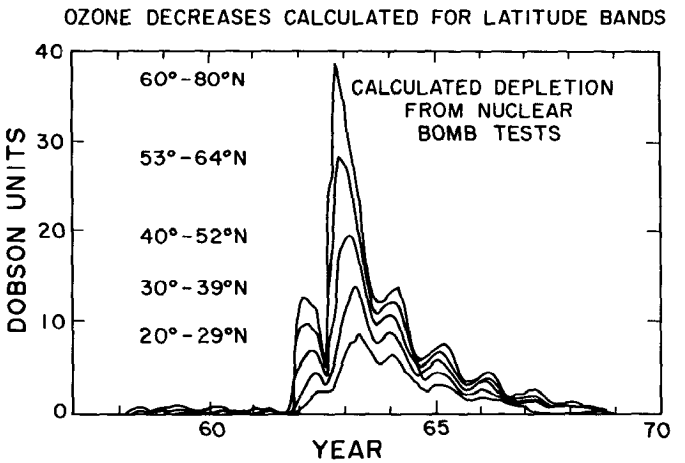

Figure 8 Calculated time-dependent ozone depletions from nuclear weapons tests in the atmosphere for northern hemisphere.

MEASUREMENTS OF ATMOSPHERIC OZONE

Regular continual measurements of ozone, which were begun in several locations during the 1920s, used the Dobson UV spectrometer. But, for various reasons, these series, including that initiated by Dobson himself (3), have not been continued to the present day without interruption. The routine measurement of ozone depends upon a null reading of the UV intensities at two wavelengths, the shorter of which is appreciably absorbed by ozone. The radiation received at the longer wavelength is attenuated in the apparatus to match that found at the shorter wavelength, thus providing a reading that can then be converted into a total amount of ozone in the air column. The readings for the particular zenith angle are then recorded as the equivalent in a vertical column after correction for the solar angle of the sun. The preferred measurement depends upon direct observation of the sun, but readings on a cloudy day are also possible from the zenith sky or from zenith clouds by careful calibration during time periods when both direct sun and zenith observations can be made. The longest, essentially continuous record from any station is that measured at Arosa, Switzerland, from August 1931 to the present. At this location, measurements of total ozone have been made on a substantial majority of the 20,000 days that have elapsed since the series was begun, and monthly averages have been recorded for all but five of the 700 months involved. The long-term monthly averages and the interannual standard deviations of the Arosa data are illustrated in Figure 1; both are generally typical of the seasonal variations found in north temperate zone locations (14).

Data have been recorded since 1931, with the ozone calculated from measurements of the C wavelength pair (311.45 nm and 332.4 nm). Since 1957, the internationally preferred ozone measurement is conducted with four wavelengths, the A and D pairs of 305.5 nm/325.4 nm and 317.6 nm/339.8 nm, to minimize any interference by scattering from aerosol particles. In principle, each pair of wavelengths should give the same ozone concentration when properly calibrated, but atmospheric path lengths are much longer during winter at high latitudes than in the tropics, and different pairs are more appropriate under each condition. Examination of long series of data for possible trends in total ozone concentration necessitates consistent recording of the data. Periodic recalibration of the basic instrument is also necessary. Such recalibrations are now conducted in side-by-side comparisons with traveling secondary standard instruments, which are maintained by comparison with an International Standard instrument. This instrument is itself recalibrated every year or two under the highly favorable conditions of the mountaintop at Mauna Loa, Hawaii (1, 4). These conditions include negligible daily spatial and tem-

poral variation in total ozone in the tropics (Figures 1 and 9), usually cloud-free sky, sun near the zenith in summer, high altitude, and unpolluted air.

In the 1957–1958 International Geophysical Year, the number of ground stations from which ozone was routinely measured was substantially increased. This increase included the establishment of several stations in Antarctica from which ozone measurements had not previously been available. An early result from Antarctica was the observation that the total ozone content over Halley Bay on the Antarctic Coast (76°S, 27°E) had a seasonal variation—after a six-month phase shift for the southern hemisphere—quite unlike that found for Spitsbergen, Norway (3). Instead of an ozone maximum near the spring equinox (see Figure 1 for Leningrad and Arosa), the Antarctic maximum occurred in mid-spring (November). Ozone concentrations in the south temperate zone (Aspendale in Figure 1) also maximize near the spring (austral) equinox. The explanation for the delayed Antarctic maximum is the existence in the southern hemisphere of an intense wintertime polar vortex in the stratosphere, such that the air over Antarctica at the beginning of winter remains there throughout the polar darkness and continues until broken up in mid-spring. Without

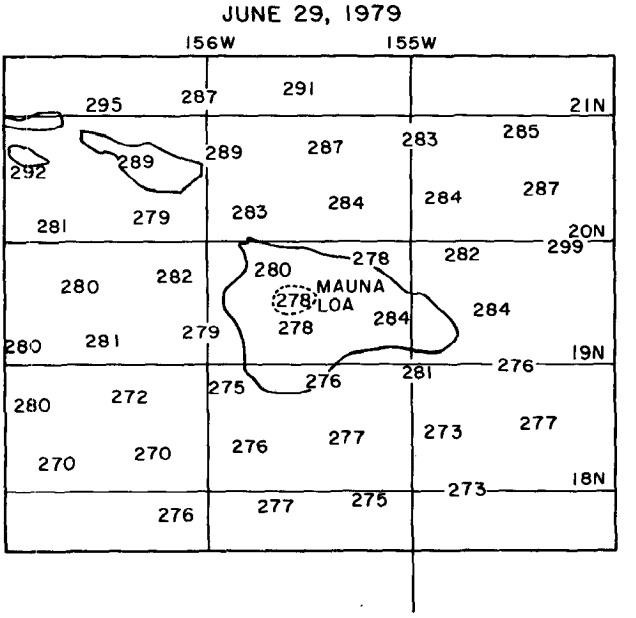

Figure 9 Total ozone measurements in vicinity of Hawaiian Islands for June 29, 1979. Dobson measurement at Mauna Loa (*dashed oval*), all others by TOMS instrument on Nimbus-7 satellite.

access to either high sun conditions or air from lower latitudes, the ozone concentration over Antarctica remains at the wintertime level until the advancing sunlight of spring heats the southern stratosphere, dissipates the vortex, and allows the arrival over the pole of lower latitude stratospheric air containing higher ozone concentrations.

When the data of Figure 1 from Arosa are divided into the periods covering the years 1931–1969 and 1970–1988, the average ozone concentrations in the more recent period are found to be less in every month (Figure 10), but especially so in the months from November through March (41). A generally similar pattern has been found for most ozone stations north of 30°N latitude, and combination of the records from various ground-level observation stations within particular latitude bands has shown a global pattern of statistically significant wintertime loss of ozone in the north temperate zone, coupled with indications of smaller losses during summer periods (Figure 11) (13, 14, 42). This differentiation in the seasonal losses of ozone had not been recognized in earlier analyses of the global Dobson ozone data (4) because the prevailing presumption from atmospheric models, which employ solely homogeneous gas phase chemistry, was that any stratospheric ozone losses would be comparable in all seasons. Consequently, the ozone data were heavily weighted in the statistical treatment toward summer observations for which the interannual variations (see Figure 1) are much smaller, and for which the signal/noise ratio of a given ozone change would then be larger (14). The current state of measurements related to atmospheric ozone has been described in 192 papers from the 1988 Ozone Symposium (43).

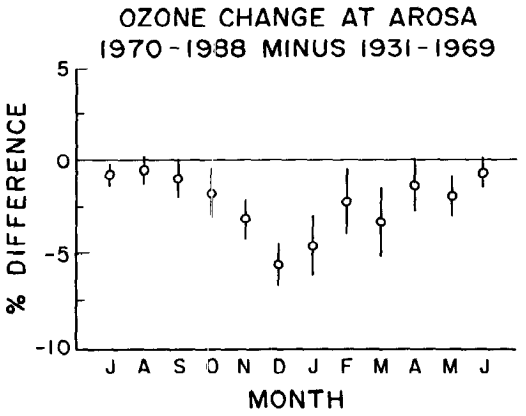

Figure 10 Percentage difference in monthly average total ozone readings at Arosa, Switzerland, for period 1970–1988 relative to 1931–1969.

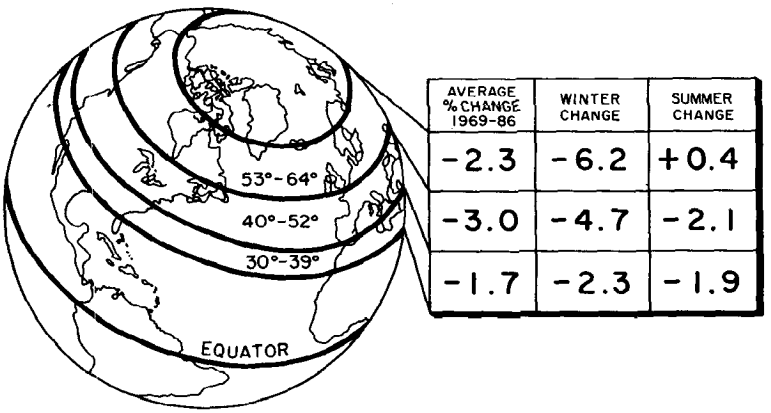

Figure 11 Percentage changes in total ozone concentrations by 1986 from average values before 1970 for latitude bands between 30°N and 64°N latitudes.

In 1970, total ozone measurements from satellites were initiated by utilizing a back-scatter ultraviolet (BUV) technique from the Nimbus-4 satellite (40). This technique depends upon differential absorption in two UV wavelengths: One is strongly sensitive to O_3, and the other is only weakly absorbed by O_3. The technique also depends upon the knowledge that most of the Earth's UV albedo depends upon interactions in the troposphere, whereas most of the ozone is in the stratosphere. Differential absorption in the stratosphere of the scattered UV radiation provides a measurement of the total atmospheric ozone, after addition in the total ozone algorithm for these satellite data of a small correction for climatologically averaged ozone for the unmeasured lower tropospheric ozone. The BUV instrument on Nimbus-4 was designed in the 1960s for a single year's ozone observations, to both explore the utility of this technique and provide a global map of the O_3 data for 1970. Excellent data were obtained over a two-year period, and fragmentary data were received for several more years as the satellite power source limped beyond its design period (40).

Two ozone-measuring instruments were included on Nimbus-7, which went into orbit in October 1978: TOMS (Total Ozone Mapping Spectrometer) and SBUV, an improved version of the original BUV device (14). The SBUV instrument focused constantly in the nadir and recorded data at many wavelengths in the UV, thereby providing both a measurement of total column ozone and some indication of its vertical distribution, because radiation at the shorter UV wavelengths is received only from stratospheric scattering. In contrast, TOMS furnished data only on total

ozone, but swung constantly through many oblique angles, as well as the nadir, thus providing hundreds of thousands of total ozone measurements daily from all latitudes except those shrouded in polar darkness.

An important limitation for decade-long trend analyses with both TOMS and SBUV was that their routine calibration relied upon daily observation of solar radiation scattered from a metallic "diffuser plate," which was slowly degraded over time from exposure to direct, unshielded solar radiation (14). The standard algorithms applied to TOMS and SBUV data corrected for most of this alteration of the diffuser plate, but accurate calibration was finally obtained by comparison of the ozone data recorded by the satellite coincident with overpasses over each ground station. The averaged data recorded by TOMS in its 14 complete orbits on June 29, 1979, are shown in Figure 9 in comparison with the single Dobson reading on Mauna Loa on that date. (Precise intercomparison includes several minor corrections, including the altitude difference between the 3400 meter height of the Mauna Loa Observatory versus the average height of the area integrated by TOMS.) Daily overpass data are available for every sunlit ground station, so that excellent statistical comparisons can be made between the ozone concentrations reported by the satellite and the Dobson stations on the ground (14).

Because the degradation of the diffuser plate on the satellite was a slow process that extended over a decade, the daily overpass data can be used to determine the validity of the data from each individual ground station, whose near-identical Dobson instruments differ widely in frequency of recalibration, care in upkeep, and skill and training of the operators. Then, over the period of a decade, comparison of the overpass data with the well-run ground stations allows a final Normalized-to-Dobson network adjustment of the algorithm used for the satellite ozone data. This cross-combination of the ground and satellite measurements provides an ozone measurement system superior to either by itself. Ultimately, however, the trend data from the combined system depends upon the constancy of behavior of the International Standard Instrument, and attempts are underway to provide a separate, on-board calibration system for the satellite instruments.

During the past two decades, careful measurements of tropospheric ozone concentrations, especially with balloon-borne ozonesondes, have shown increases as large as 5–10% per year in both Europe and North America (44, 45). Comparisons with French data from 1870–1890, validated by current duplication of the century-old experimental procedures, have shown that the average ground-level ozone concentrations in rural areas are now about double what they were in the late 1800s (46, 47). Moreover, the maximum in O_3 concentration now arrives in mid-summer,

rather than early spring, which is consistent with solar-induced photochemistry as the prime cause of the change. These ozone increases in the troposphere tend to mask stratospheric depletion in measurements by Dobson spectrometers, which simply record the total ozone independent of altitude. In contrast, the TOMS satellite measurements of total ozone are not sensitive to concentration changes in the lower troposphere, which occur below the altitudes of primary importance for outward scattering of solar UV radiation. For this reason, intercomparisons between trends determined from the Dobson network and TOMS require very careful analysis of possible influences of variations near the Earth's surface. Comparable, century-old tropospheric data from the southern hemisphere are not available, but the ozone increases from photochemical smog should be confined to areas with relatively high concentrations of both hydrocarbons and NO_x.

ANTARCTIC OZONE LOSS

The total amount of ozone over the Halley Bay, Antarctica, Dobson station decreased sharply in the 1980s (48) during the first month of spring (October). The amount dropped from an average of about 310 Dobson Units (DU) in the decade beginning in 1957 to less than 200 DU by 1984 (Figure 12) and as low as 160 DU by the end of the 1980s (14). The geographic extent of this ozone loss has been vividly illustrated through the comprehensive coverage of TOMS on Nimbus-7, which has documented that the decline is initiated in late August, as the sunlight of approaching spring first penetrates the polar darkness, and is essentially completed each year by the first week in October, as shown in Figure 13 (13, 14). The area of substantial ozone loss extends from the south pole to about 60°S latitude (Figure 14) or about one fifteenth of the entire surface area of the Earth. The daily minimum values of ozone recorded by TOMS are given in Figure 13 for 1979 and 1987–1990 (14, 49). Clearly, the loss of ozone shows seasonal and interannual structure that reflects the complex Antarctic meteorology.

In 1987, 1989, and 1990, the total global supply of ozone was diminished by about 3% in one month through losses in the south polar stratosphere. This region of greatly diminished ozone remains over Antarctica until the break-up of the polar vortex in mid- to late November, and then patches of ozone-depleted air move northward and gradually dissipate into the rest of the global stratosphere. In December 1987, stratospheric air depleted in ozone over the Antarctic drifted northward over Melbourne (Aspendale), Australia, thus bringing the lowest December readings (270 DU for several weeks) yet recorded there (50). Because stratospheric ozone is constantly

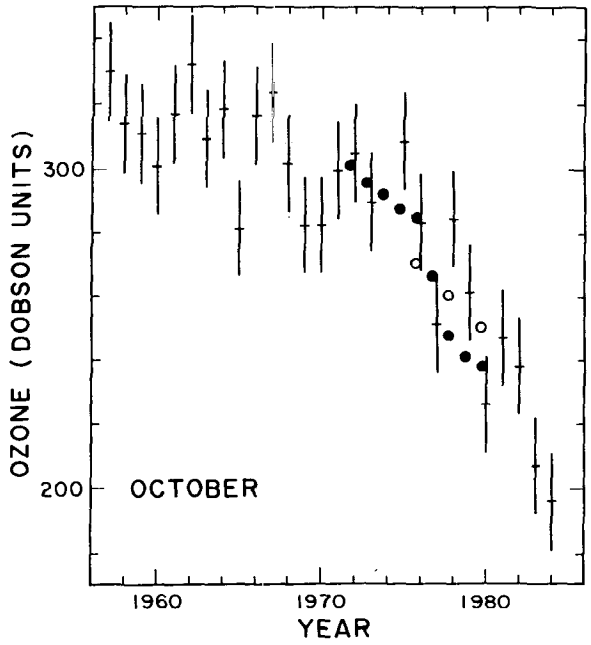

Figure 12 Average October total ozone concentrations over Halley Bay, Antarctica (76°S, 27°E) for 1957–1984. The circles represent observed concentrations of CFC-11 and CFC-12, graphed with higher levels to the bottom to illustrate a correlation with ozone depletion.

being both created and destroyed in a dynamic photochemical equilibrium, these depleted air masses gradually build again toward their normal ozone values, only to have another massive loss occur during the following Antarctic spring. The TOMS data, when normalized to the Dobson ground network, show measurable ozone depletion at all latitudes with the larger losses in the two polar regions.

Both the Dobson and TOMS systems provide data only on the total column of ozone without regard to its altitude and, therefore, cannot identify which altitudes are most depleted. However, ozonesondes (balloons carrying an electrochemical sensor for atmospheric ozone) have been flown on a regular basis for more than 30 years, many of the programs having also been initiated during the International Geophysical Year. These instruments have shown that the Antarctic ozone loss is heavily concentrated in the lower stratosphere between about 14 and 24 km altitude (Figure 15). In some air masses at these altitudes, which normally carry the greatest mixing ratios of ozone, essentially all of the ozone is

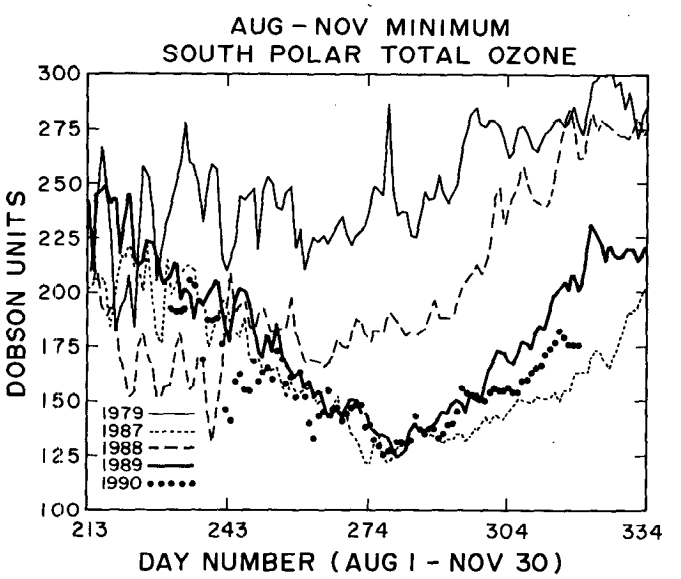

Figure 13 Daily minimum total ozone concentration recorded by TOMS satellite instrument south of 60°S latitude for August to November in 1979, 1987, 1988, 1989, and 1990.

chemically removed within a period of about 4–6 weeks, as illustrated by the 15 km altitude region with the November 5, 1987, ozonesonde of Figure 15. The balloon-borne data have been corroborated by measurements from another satellite instrument, SAGE II, which looks directly at the sun as it rises or sets for the orbiting spacecraft and provides about 30 vertical ozone profiles per day spread over the latitude range from 80°N to 80°S (51, 52). In Figure 16, the close intercomparison between vertical ozone profiles from an ozonesonde launched from Halley Bay and the Antarctic SAGE II data for the same day confirms the precision of both systems. With initial O_3 mixing ratios as high as 2 ppmv, corresponding to 4×10^{12} molecules/cm^3, the maximum loss rate for ozone must then be about 10^{11} molecules O_3/day. With ClO concentrations of 1 ppbv, or 2×10^9/cm^3, the chain reaction efficiency must be sufficient for each ClO chain to eliminate 50 O_3/molecules per day, or one every 30 minutes, and maintain this rate for six weeks.

CHLORINE CHEMISTRY IN THE ANTARCTIC STRATOSPHERE

The major losses of ozone during the Antarctic spring were not predicted by the existing atmospheric models, nor once the phenomenon was known

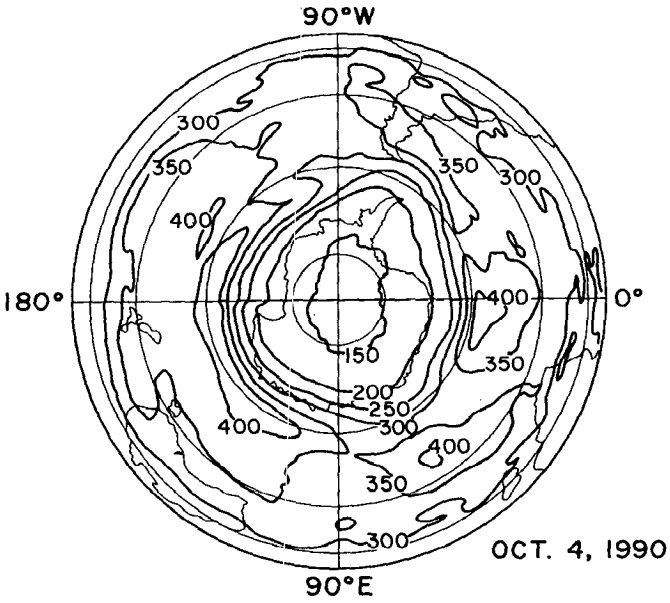

Figure 14 TOMS total ozone readings for the southern hemisphere on October 4, 1990. Heavy lines, ozone contours in Dobson units. Light lines for 80°, 60°, 40°, and 20°S latitudes and for major land masses.

were they susceptible to successful simulation as long as the chemical reaction sequences were limited to homogeneous gas phase reactions (53). Three special US expeditions to the Antarctic were organized: two of them, in 1986 and 1987, operated from the US base at McMurdo; the third, in 1987, employed both ER-2 and DC-8 aircraft flying from Punta Arenas, Chile. Antarctic ozone was described in 45 papers in a special issue of *Geophysical Research Letters* (54) and again in 62 papers in two dedicated issues of the *Journal of Geophysical Research* (55). The combined results of these three expeditions, together with other experiments, provide a comprehensive understanding of the ozone-related chemistry of the Antarctic stratosphere. This chemistry responds to the special meterological and physical conditions of the polar vortex. Air maintained in complete darkness continues to radiate to space in the infrared wavelengths, thus becoming colder and colder. When the temperature falls to about $-78°C$, the condensation point has been reached for crystals of nitric acid trihydrate, $HNO_3 \cdot (H_2O)_3$, (NAT), and these appear as PSCs (Type I) with roughly spherical drops in the 1 μm size range (56, 56a). A further decrease of another five or six degrees causes the further condensation of water ice

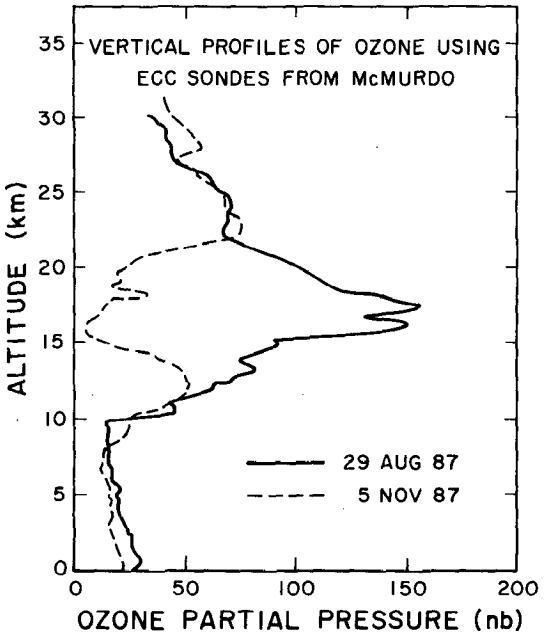

Figure 15 Vertical distribution of ozone as measured over McMurdo, Antarctica, by balloon-borne electrochemical sensors in late winter (Aug. 29) and mid-spring (Nov. 5).

on the existing crystals, thus forming PSC Type II clouds with larger, amorphous shapes (57, 58). Both types of clouds furnish particulate surfaces capable of supporting heterogeneous catalytic reactions between compounds whose gas phase homogeneous reaction rates are effectively zero.

The existence of the clouds has been demonstrated by variations in the emission from the atmosphere to an overhead satellite of 1 μm infrared radiation, with information about the particle shapes deduced by probing the stratosphere with polarized infrared radiation and measuring the degree of depolarization in the return (56, 56a). Additional particulate material is periodically introduced into the stratosphere by volcanic explosions, the two most prominent being St. Helen's in 1980 and El Chichon in April 1982. The PSCs produce increases in optical depth, measured at 1.06 μm from 10^{-3} to about 10^{-2} in the Antarctic (Figure 17) before and after the El Chichon eruption (volcanic eruptions are shown with vertical arrows). Mid-winter spikes in optical depth appear in the Arctic in 1980 and 1981, and then reappear over the El Chichon background in 1986. The effects of

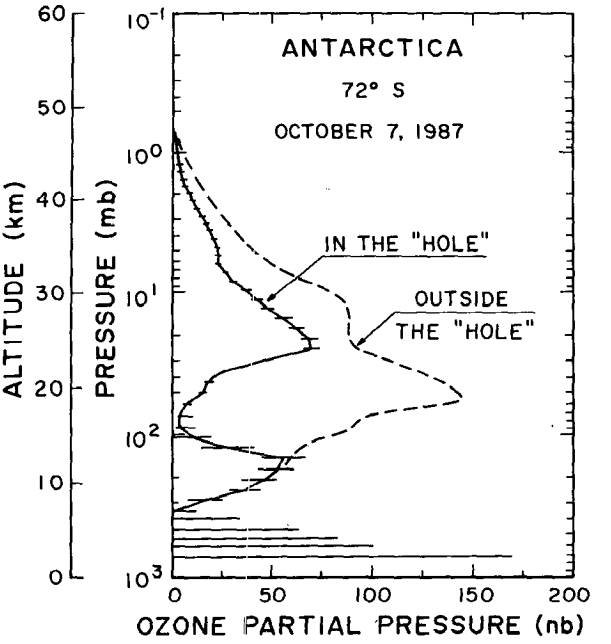

Figure 16 Vertical distribution of ozone as measured by SAGE II instrument on ERBS satellite (*horizontal bars*) on October 7, 1987, at 72°S versus ozonesonde measurement from Halley Bay, Antarctica, on the same day (*solid line*) and typical ozonesonde data in mid-August.

El Chichon gradually faded away during the late 1980s, and the particulate polar concentrations were almost back to the levels observed in the pre-1982 stratosphere prior to the Pinatubo eruption in June, 1991.

The heterogeneous reactions on PSC surfaces have two consequences of prime importance (58–62). As also occurs in other latitudes, the daylight nitrogen oxides, NO and NO_2, are always converted in darkness, first by reaction with O_3 to form NO_3 and then with another NO_2 molecule to form N_2O_5. In the presence of PSCs, this sequence is pushed further as N_2O_5 reacts with H_2O on the particle surfaces to form nitric acid, which is then sequestered in the cloud as NAT. As these particles grow in size, they can become heavy enough to fall under gravitational forces and both denitrify and dehydrate the air mass in which they form. Even without gravitational separation, effectively all of the nitrogen oxides can be trapped in the cloud particles, unable to participate in gaseous reactions.

Several chemical reactions involving chlorinated molecules are also catalyzed by the particulate surfaces of the PSCs, including Equations 20 and

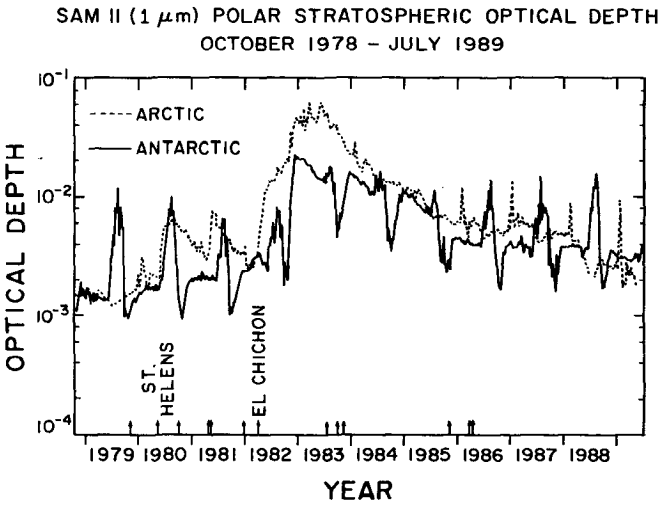

Figure 17 Optical depth at 1 μm in polar regions, as measured by SAM II, October 1978–July 1989.

21. Again, the nitric acid is incorporated into the PSCs, but both Cl_2 and HOCl escape from the surfaces back into the gas

$$HCl + ClONO_2 \rightarrow Cl_2 + HNO_3 \qquad 20.$$

$$H_2O + ClONO_2 \rightarrow HOCl + HNO_3 \qquad 21.$$

phase. These reactions were shown to take place very rapidly on various nominally inert laboratory surfaces (62), and incorporation of these reactions into atmospheric models in 1984 had already indicated potentially very large increases in estimates of future stratospheric ozone depletion (36). However, the key question for semi-quantitative application to atmospheric calculations was whether such reactions could occur on ice surfaces and, if so, with what magnitude accommodation coefficient. Conventional wisdom indicated coefficients in the 10^{-5} to 10^{-6} range, at which the rates of conversion of HCl and $ClONO_2$ into more photosensitive compounds would be unimportant for the stratospheric context. However, careful laboratory experiments demonstrated that the accommodation coefficients for both Equations 20 and 21 were in the range of 0.1–0.01 (58–60) and, therefore, of major importance for the atmosphere.

Molecules such as H_2O, N_2O_5, Cl_2O, HOCl, $ClONO_2$, and HNO_3 can all be described as X-O-Y molecules with X or Y = Cl, H, or NO_2 (61). All of these appear to react rapidly with exchange of substituents on catalytic surfaces, and to react with HCl as well. These surface alterations

of the usual distributions among nitrogenous and chlorinated molecules are completed in the polar darkness, thus providing a very different redistribution of chemicals for exposure when the first sunlight of the late Antarctic winter begins to penetrate the polar darkness. Both Cl_2 and HOCl photolyze almost immediately, and the Cl atoms react rapidly with O_3 to form ClO, as they do in the tropic and temperate stratosphere. However, in the absence of NO_2—with the N sequestered in the PSCs as HNO_3—the normal diversion of ClO into the temporary reservoir $ClONO_2$ cannot occur. At the same time, the formation of HCl by reaction of Cl with CH_4 is substantially slowed by the low temperatures.

With the usual chain-breaking reservoir formation greatly suppressed by these chemical alterations, the radical ClO can survive for much longer periods of time and build to stratospheric concentrations much higher than those found in the tropical and temperate stratosphere. However, the scarcity of O atoms, with the long solar path lengths available early in the Antarctic spring, prevent the completion of the chain of Equation 8 of the usual ClO_x sequence. Without either NO_2 or O as reaction partner, ClO can then react with other free radicals, in particular the dimerization reaction of Equation 22 (63), combination with HO_2 by Equation 23 (53), or with BrO in Equation 24 (64). The latter reaction releases both Cl and Br in atomic form, and each can then react again with O_3 to reform ClO and BrO.

$$ClO + ClO + M \rightarrow ClOOCl + M \qquad 22.$$

$$ClO + HO_2 \rightarrow HOCl + O_2 \qquad 23.$$

$$ClO + BrO \rightarrow Cl + Br + O_2. \qquad 24.$$

The sum of these processes is then a chain reaction conversion of two molecules of O_3 into three molecules of O_2, which operate without the O atom steps of the chain reactions characteristic of the temperate and tropical stratosphere. The ClOOCl and HOCl molecules formed in Equations 22 and 23 are readily photolyzed with the release of two Cl atoms and Cl + HO, respectively. Again, chain cycles are completed that correspond to the conversion of two molecules of O_3 into three of O_2. Current calculations indicate that the ClOOCl dimer route is the dominant chain reaction in the Antarctic stratosphere (58, 65, 65a, 66), with the BrO/ClO reaction also playing a significant role and only minor importance for ClO reactions with HO_2 or O.

Confirmation of the qualitative chemical ideas postulated for the Antarctic stratosphere has been provided by the Antarctic expeditions, and the data are both abundant and accurate enough for quantitative evaluation of the ozone loss through the Antarctic spring of 1987. The concentrations

of ClO attained levels as high as 1.3 ppbv in the altitude range near 18 km, thus providing concentrations high enough to make the ClO dimerization of Equation 22 the major removal process for ClO radicals. (The atmospheric chlorine concentration summed over all chemical forms was less than 1.3 ppbv until the early 1970s, as shown in Figure 4, thereby explaining why the massive springtime ozone losses over Antarctica did not appear until the late 1970s.)

The most striking observations of the Antarctic experiments were those provided by the simultaneous measurement from the ER-2 aircraft at 18 km altitude of the concentrations of ClO and O_3 (65, 65a). Results from ER-2 flights on three different days are shown in Figure 18. On August 23, soon after the ending of the winter darkness at 72°S latitude, a sharp rise in ClO concentration after entering the polar vortex was observed, with little change in O_3 concentrations. By September 21, the increased ClO concentration in the vortex was now accompanied by a very large decrease in ozone—a loss of 80% in one month. The earlier September 16 data not only show a large decrease in ozone within the vortex, but because the vortex edge was rather ragged, demonstrate a strong ClO/O_3 anticorrelation through many increases and decreases of each.

Atmospheric model calculations indicate relatively little transport to the northern hemisphere of ozone-depleted air from the south polar region. However, polar stratospheric clouds also appear in the north polar region (Figure 17), although not with the intensity and regularity found in the south (56, 56a). Experiments performed by both ground-based and aircraft expeditions into the Arctic have demonstrated that chemical conditions exist that closely resemble the Antarctic ozone depletion situation, with ClO concentrations exceeding 1 ppbv (67), and that rapid ozone loss has

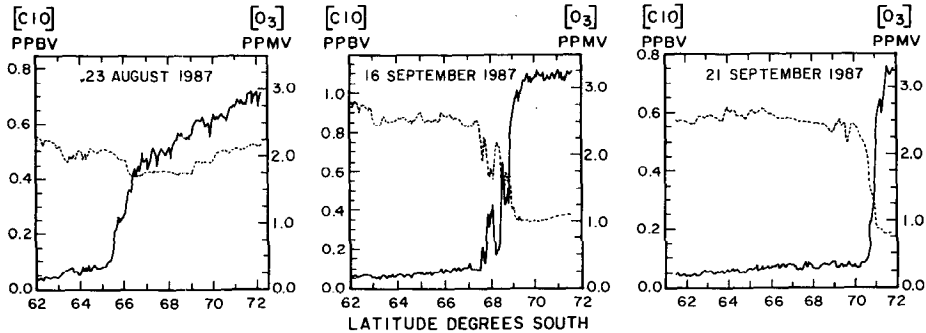

Figure 18 ClO and O_3 measurements at 18 km over Antarctica in 1987: August 23, September 16, September 21.

occurred for a few days in specific air masses (68). The Arctic polar vortex is, however, much weaker than in the Antarctic, and most air masses oscillate out of the north polar darkness within a week or two, only to be replaced by another air mass in which PSCs can form and ozone depletion can occur. The stratospheric meteorology of the Arctic (69) is also susceptible to "sudden warming." In 1989, temperature measurements on sounding balloons showed that the stratospheric temperature minimum over Berlin rose from −80°C on February 1 to 0°C on February 10 and was accompanied by comparable increases over most of the polar regions, as the cold Arctic air was displaced by warmer air from the south. After most sudden warmings, the Arctic stratosphere usually does not get cold enough again during that winter for the formation of further PSCs. Nevertheless, significant ozone losses have been recorded in north polar air masses (70, 71), and it is likely that such polar losses contribute significantly to the total ozone losses recorded in the wintertime by the Dobson network. The Airborne Arctic Stratosphere Expedition (AASE) in early 1989 has been described in 63 articles in a special issue of *Geophysical Research Letters* (70).

Ozone losses from the temperate/tropical ClO chain of Equations 7 and 8 are predicted to maximize in the upper stratosphere near 40 km, whereas the polar ClO chain operates chiefly in the 20 km region. Vertical profile measurements by SAGE II and the Dobson umkehr technique (measurements as sunset approaches) have both shown decreases in ozone at 40 km over the past decade (Figure 19), which are in rough agreement with the calculated losses and with each other (14). The accuracy of the vertical ozone profiles by the SAGE II technique is still excellent at 20–25 km, and the losses indicated at 25 km in Figure 19 are not predicted by atmospheric models that use homogeneous gas phase reactions alone. These temperate zone measurements suggest that ozone losses are also being observed at these altitudes outside the polar regions. The existence of volcanic particulates, and of sulfuric acid aerosol during quiescent volcanic periods, provides surfaces on which chemical catalysis can also occur (72, 73). Contributions to observed ozone loss at 20 km in the temperature zone can be attributed to either in situ loss or transport from the polar regions, and the relative importance of each remains to be assessed.

MAJOR CONSEQUENCES OF STRATOSPHERIC OZONE DEPLETION

The depletion of stratospheric ozone can have two major physical consequences in the atmosphere, both of which are ultimately concerned with

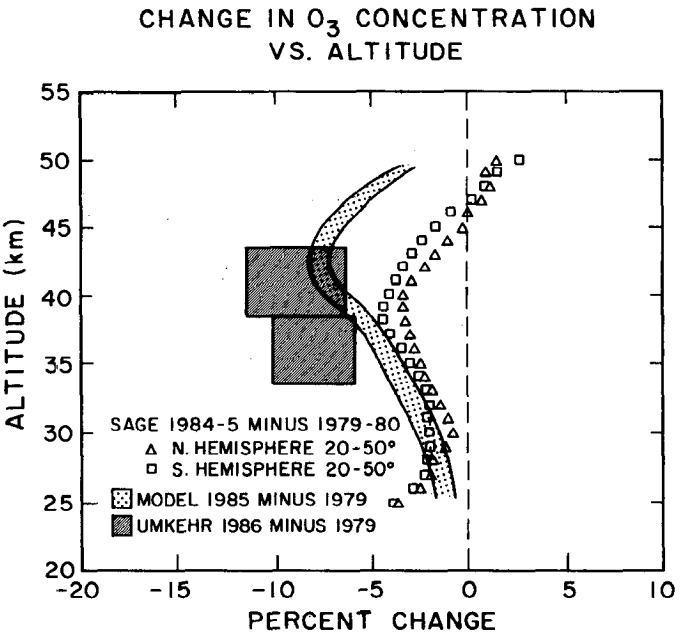

Figure 19 Changes in ozone versus altitude, as calculated by atmospheric models and measured by SAGE II versus SAGE I and by Dobson umkehr.

the role of O_3 in absorption of UV radiation. The absorption of UV radiation by O_3 in Equation 3 is usually followed by recombination in Equation 2, with the result that the incoming solar energy is converted into heat at the altitude at which absorption takes place. This conversion of UV energy into heat is the ultimate cause for the existence of the stratosphere itself, because a heat source in the upper stratosphere is necessary to maintain the higher temperature at 50 km than at 20 km. Although the UV absorption cross sections of O_3 in the 220–290 nm range are sufficiently strong (4) to ensure that atmospheric absorption would still occur even with 50% reduction in ozone, lesser ozone concentrations in the upper stratosphere decrease the strength of the heat source at those altitudes and are expected to lead to lower temperatures from about 40 km up to the stratopause at 50 km (74). For these UV wavelengths, the important factor is not necessarily how much ozone there is in a total vertical column, but the vertical profile of the ozone distribution, especially in the higher altitudes. A redistribution toward lower altitudes of the same total amount of ozone results in an altered temperature gradient, with less heat introduced above and more below. Satellite observations of

stratopause temperatures indicate a global average decrease of 1.7 ± 1.0 K over the past decade (14). The increased absorption of terrestrial infrared radiation by CO_2 and other trace gases—the greenhouse effect—is also expected to make an additional smaller contribution to cooling at the stratopause. The combined predicted temperature loss is consistent with the observations.

The other major effect is concerned with UV radiation with wavelengths between about 280–320 nm, which is frequently designated as "UV-B," in contrast to UV-A (320–400 nm) and UV-C (shorter than 280 nm). In this region, the normal amount of O_3 is sufficient to cause only partial atmospheric absorption, with the remainder penetrating to the surface. Lesser amounts of total ozone then allow transmission of higher percentages of UV-B to the surface and to all biological species exposed to solar radiation at the surface. Direct measurements of atmospheric penetration by UV-B have been made in only a few locations, but the standard Dobson instrument measurement of ozone is actually a physical measurement of the relative penetration of a UV-B wavelength (e.g. 311.45 nm) versus a UV-A wavelength (e.g. 332.4 nm). In the latter instance, a measurement of an increase in the ratio of radiation received at the instrument at 311.45 nm versus 332.4 nm is reported as a decrease in total column ozone. Because no indication exists that UV-A (or visible) solar radiation has changed even as much as 0.1% over time, Dobson instrument reports of reduced ozone concentrations represent observations of increased levels of UV-B radiation.

Measurements of UV-B radiation have been reported with Robertson-Berger UV monitors in the United States (75), Switzerland (76), and Australia (77). Figure 20 illustrates the 24-hour response of one such instrument at Bismarck, North Dakota, for June 20 and for several days in April, including the arrival on April 19 of thick clouds that reduced daytime UV-B intensities nearly to zero. The wintertime UV-B exposures in Bismarck are reduced from the summertime values by a factor of almost 20. Unlike the strongly collimated Dobson instruments, which measure direct UV transmission from the sun at particular wavelengths, the Robertson-Berger meters integrate over a 180° acceptance angle, with a wavelength weighting factor set to mimic the erythemal (sunburn) response of human skin. Such an instrument located at the Jungfraujoch in the Swiss Alps has recorded an increase in UV-B radiation over the past decade (76), in basic agreement with the Dobson instrument indications of reduced ozone concentrations. In contrast, the US-based instruments have, for the most part, recorded slight reductions in total UV-B since 1974 (70). Because these instruments are generally located in semi-urban areas, the known increase in tropospheric ozone may have reduced the amount

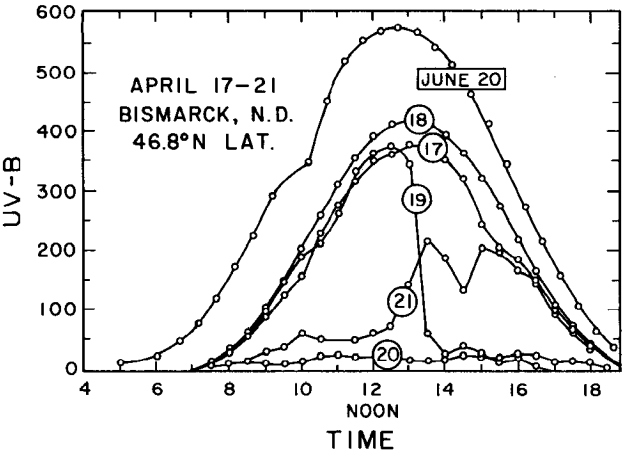

Figure 20 UV-B readings for six days in Bismarck, North Dakota: June 20 and April 17–21.

of scattered UV-B radiation that arrived along horizontal paths to the instrument at the same time that direct UV-B radiation was on an increase (78). The measurements in Australia coincided with a marked decrease in stratospheric ozone from the break-up of the Antarctic ozone hole of 1987 (50, 77). In this instance, the measured UV-B under clear sky conditions showed the expected marked increase; however, a presumably fortuitous increase in average cloudiness over the same period reduced the number of hours of major UV-B exposure, so that the total UV-B was essentially unchanged (77).

The most important direct consequences for humans of an increased UV-B exposure are believed to involve the various types of skin cancer, eye cataracts, and possibly deterioration of the immune response system (79–81). Studies of other biological systems have indicated that many of these are also under UV-B pressure in the natural surroundings. Further discussion of these potential biological responses is beyond the scope of this review.

REGULATION OF GLOBAL CFC EMISSIONS

Controls on emissions of CFCs to the atmosphere were first announced in 1976 in the US, and were then extended to Canada, Norway, and Sweden in the late 1970s (24). These controls applied only to their application as propellant gases in aerosol sprays, but not to other uses as refrigerants,

plastic foam-blowing agents, or cleaning agents for electronics. An international agreement, which was reached in Montreal in September 1987, called for 50% reduction in yearly emissions by 1999. This Montreal Protocol was strengthened in London in June 1990 to bring about complete cessation of CFC emissions by the end of the century. Figure 4 illustrates the extrapolated values of organochlorine concentrations in the troposphere for continued emission at 1986 levels, the reduced emissions under the Montreal Protocol of 1987, and the elimination of CFC release by the year 2000. The very long atmospheric lifetimes for the CFCs ensure that the organochlorine concentration will decrease only very slowly, thus continuously supporting stratospheric ozone depletion during the twenty-first and twenty-second centuries. An entire issue of the Swedish journal *Ambio* was devoted to the scientific and regulatory problems associated with ozone depletion by chlorofluorocarbons (82).

ACKNOWLEDGMENTS

Research in chlorocarbon chemistry at the University of California Irvine has been supported by several agencies, with major contributions by Department of Energy Contract No. DE-FG03-86ER-13469 and National Aeronautics and Space Administration Contract No. NAGW-452, and their precursors.

Literature Cited

1. Hartley, W. N. 1881. *J. Chem. Soc.* 39: 57–61
2. Hartley, W. N. 1881. *J. Chem. Soc.* 39: 111–28
3. Dobson, G. M. B. 1968. *Appl. Optics* 7: 387–405
4. World Meteorol. Organ./Natl. Aeronaut. Space Adm. 1986. *Atmospheric Ozone 1985. WMO Global Ozone Research and Monitoring Project, Rep. No. 16. 3 Vols.* 1150 pp.
5. Chapman, S. 1930. *Mem. R. Meteorol. Soc.* 3: 103–25
6. Crutzen, P. J. 1971. *J. Geophys. Res.* 76: 7311–27
7. Johnston, H. S. 1971. *Science* 173: 517–22
8. Stolarski, R., Cicerone, R. J. 1974. *Can. J. Chem.* 52: 1610–15
9. Molina, M. J., Rowland, F. S. 1974. *Nature* 249: 810–12
9a. Rowland, F. S., Molina, M. J. 1975. *Rev. Geophys. Space Phys.* 13: 1–35
10. Bauer, E., Gilmore, F. R. 1975. *Rev. Geophys. Space Phys.* 13: 451
10a. Chang, J. S., Duewer, W. H., Wuebbles, D. J. 1979. *J. Geophys. Res.* 84: 1755–65
11. Natl. Acad. Sci. 1975. *Environmental Impact of Stratospheric Flight.* Washington, DC
11a. Climatic Impacts Assess. Program (CIAP) Monogr. 1. 1975. *The Natural Stratosphere of 1974*, ed. A. J. Grobecker. US Dep. Transp., DOT-TST-75-51, Washington, DC
12. Makide, Y., Rowland, F. S. 1981. *Proc. Natl. Acad. Sci. USA* 78: 5933–37
13. World Meteorol. Organ. 1990. *Scientific Assessment of Stratospheric Ozone: 1989, Vol. 1.* NASA/UKDOE/NOAA/UNEP/WMO. 486 pp.
14. World Meteorol. Organ. 1990. *Report of International Ozone Trends Panel 1988. WMO Rep. No. 18.* 2 Vols. 987 pp.
15. DeMore, W. B., Sander, S. P., Golden, D. M., Molina, M. J., Hampson, R. F., et al. 1990. *Chemical Kinetics and Photochemical Data for Use in Stratospheric Modeling, Evaluation Number 9. Jet Propulsion Laboratory 90-1.* 217 pp.
16. Jones, R. L., Pyle, J. A., Harries, J. E.,

Zavody, A. M., Russell, J. M. III, Gille, J. C. 1986. *QJR Meteorol. Soc.* 112: 1127–43
16a. Hansen, A. R., Robinson, G. D. 1989. *J. Geophys. Res.* 94: 8474–84
17. Blake, D. R., Rowland, F. S. 1988. *Science* 239: 1129–31
17a. Khalil, M. A. K., Rasmussen, R. A. 1990. *Environ. Sci. Technol.* 24: 549–53
18. Craig, H., Chou, C. C. 1982. *Geophys. Res. Lett.* 9: 1221–24
18a. Rasmussen, R. A., Khalil, M. A. K. 1984. *J. Geophys. Res.* 89: 11599–605
19. Chappelaz, J., Barnola, J. M., Raynaud, D., Korotkevich, Y. S., Lorius, C. 1990. *Nature* 345: 127–31
20. Cicerone, R. J., Oremland, R. S. 1988. *Glob. Biogeochem. Cycles* 2: 299–327
21. Weiss, R. F. 1981. *J. Geophys. Res.* 86: 7185–95
22. Muzio, L. J., Kramuch, J. C. 1988. *Geophys. Res. Lett.* 15: 1369–72
23. Linak, W. P., McSorley, J. A., Hall, R. E., Ryan, J. V., Srivastava, R. K., et al. 1990. *J. Geophys. Res.* 95: 7533–41
24. Rowland, F. S. 1990. *Ambio* 19: 281–92
25. Cunnold, D. M., Prinn, R. G., Rasmussen, R. A., Simmonds, P. G., Alyea, F. N., Cardelino, C. A., et al. 1986. *J. Geophys. Res.* 91: 10797–817
26. Crutzen, P. J., Isaksen, I. S. A., McAfee, J. R. 1978. *J. Geophys. Res.* 83: 345–63
27. Wilson, S. R., Crutzen, P. J., Schuster, G., Griffith, D. W. T., Helas, G. 1988. *Nature* 334: 689–91
28. Zander, R., Gunson, M. R., Foster, J. C., Rinsland, C. P., Namkung, J. 1990. *J. Geophys. Res.* 95: 20519–25
29. Singh, H. 1977. *Geophys. Res. Lett.* 4: 101–4
30. Prinn, R., Cunnold, D., Rasmussen, R., Simmonds, P., Alyea, F., et al. 1987. *Science* 238: 945–50
31. Derwent, R. G., Volz-Thomas, A. 1990. *Scientific Assessment of Stratospheric Ozone: 1989*, Vol. 2, pp. 127–46
32. Prather, M. 1990. *Scientific Assessement of Stratospheric Ozone: 1989*, Vol. 2, pp. 149–62
33. Fisher, D. A., Hales, C. H., Filkin, D. L., Ko, M. K. W., Sze, N. D., et al. 1990. *Nature* 344: 508–12
34. World Meteorol. Organ. 1990. *Scientific Assessment of Stratospheric Ozone: 1989*. Vol. 2. AFEAS Rep. 515 pp.
35. Solomon, S., Tuck, A. 1990. *Nature* 348: 203
36. Rowland, F. S. 1989. *Am. Sci.* 77: 36–47
37. Johnston, H. S., Kinnison, D. E., Wuebbles, D. J. 1989. *J. Geophys. Res.* 94: 16351–63
38. Turco, R. P., Toon, O. B., Ackerman, T. P., Pollack, J. B., Sagan, C. 1983. *Science* 222: 1283–97
39. Thompson, S. L., Ramaswamy, V., Covey, C. 1987. *J. Geophys. Res.* 92: 10942–60
40. Natl. Acad. Sc. 1976. *Halocarbons: Effects on Stratospheric Ozone*. Panel on Atmospheric Chemistry. 352 pp.
41. Harris, N. R. P., Rowland, F. S. 1991. *J. Geophys. Res.* In press
42. Rowland, F. S., Harris, N. R. P., Bojkov, R. D., Bloomfield, P. 1989. In *Ozone in the Atmosphere*, ed. R. D. Bojkov, P. Fabian, pp. 71–75. Hampton, Va: Deepak
43. *Ozone in the Atmosphere*, Proc. Quadrennial Ozone Symp., 1988 and Tropospheric Ozone Workshop, 1989. Hampton, Va: Deepak. 822 pp.
44. Logan, J. A. 1985. *J. Geophys. Res.* 90: 10463–82
45. Low, P. S., Davies, T. D., Kelly, P. M., Farmer, G. 1990. *J. Geophys. Res.* 95: 22441–53
46. Volz, A., Kley, D. 1988. *Nature* 332: 240–42
47. Volz, A., Geiss, H., McKeen, S., Kley, D. 1989. In *Ozone in the Atmosphere*, Proc. of the Quadrennicl Ozone Symp. 1988 and Tropospheric Ozone Workshop, pp. 447–50. Hampton, Va: Deepak
48. Farman, J. C., Gardiner, B. G., Shanklin, J. D. 1985. *Nature* 315: 207–10
49. Herman, J. R., Hudson, R., McPeters, R., Stolarski, R., et al. 1991. *J. Geophys. Res.* 96: 7531–45
50. Atkinson, R. J., Matthews, W. A., Newman, P. A., Plumb, R. A. 1989. *Nature* 340: 290–93
51. Osborn, M. T., Rosen, J. M., McCormick, M. P., Wang, P.-H., Livingston, J. M., Swissler, T. J. 1989. *J. Geophys. Res.* 94: 8353–66
52. Attmannspacher, W., de la Noe, J., de Muer, D., Lenoble, J., Megie, G., et al. 1989. *J. Geophys. Res.* 94: 8461–66
53. Solomon, S., Garcia, R. R., Rowland, F. S., Wuebbles, D. J. 1986. *Nature* 321: 755–57
54. Antarctic Ozone. 1986. Nov. Suppl., *Geophys. Res. Lett.* 13: 1191–1362
55. Airborne Antarctic Ozone Experiment (AAOE) 1989. *J. Geophys. Res.* 94: 11181–737, 16437–860
56. McCormick, M. P., Steele, H. M., Hamill, P., Chu, W. P., Swissler, T. J. 1982. *J. Atmos. Sci.* 3: 1387–97
56a. McCormick, M. P., Trepte, C. R. 1986. *Geophys. Res. Lett.* 13: 1276–79
57. Hanson, D. R., Mauersberger, K. 1988. *J. Phys. Chem.* 92: 6167–70

57a. Hanson, D. R. 1990. *Geophys. Res. Lett.* 17: 421–23
58. Solomon, S. 1990. *Nature* 347: 347–54
59. Molina, M. J., Tso, T.-L., Molina, L. T., Wang, F. C. Y. 1987. *Science* 238: 1253–57
60. Tolbert, M. A., Rossi, M. J., Malhotra, R., Golden, D. M. 1987. *Science* 238: 1258–60
61. Rowland, F. S. 1988. In *The Changing Atmosphere*, ed. F. S. Rowland, I. S. A. Isaksen, pp. 121–40. London: Wiley
62. Rowland, F. S., Sato, H., Khwaja, H., Elliott, S. M. 1986. *J. Phys. Chem.* 90: 1985–88
63. Molina, L. T., Molina, M. J. 1987. *J. Phys. Chem.* 91: 433–36
64. McElroy, M. B., Salawitch, R. J., Wofsy, S. C., Logan, J. A. 1986. *Nature* 321: 759–62
65. Anderson, J. G., Brune, W. H., Proffitt, M. H. 1989. *J. Geophys. Res.* 94: 11465–79
65a. Anderson, J. G., Toohey, D. W., Brune, W. H. 1991. *Science* 251: 39–46
66. Barrett, J. W., Solomon, P. M., deZafra, R. L., Jaramillo, M., Emmons, L., Parrish, A. 1988. *Nature* 336: 455–58
67. Brune, W. H., Toohey, D. W., Anderson, J. G., Chan, K. R. 1990. *Geophys. Res. Lett.* 17: 505–8
68. Salawitch, R., McElroy, M. B., Yatteau, J. H., Wofsy, S. C., Schoeberl, M. R., et al. 1990. *Geophys. Res. Lett.* 17: 561–64
69. Labitzke, K. 1987. *Geophys. Res. Lett.* 14: 535–37
70. Airborne Arctic Stratosphere Expedition (AASE) 1990. *Geophys. Res. Lett.* 17: 313–564
71. Fahey, D. W., Kelly, K. K., Kawa, S. R., Tuck, A. F., Loewenstein, M., et al. 1990. *Nature* 344: 321–24
72. Hofmann, D. J., Solomon, S. 1989. *J. Geophys. Res.* 94: 5029–41
73. Arnold, F., Buhrke, Th., Qiu, S. 1990. *Nature* 348: 49–50
74. Lacis, A. A., Wuebbles, D. J., Logan, J. A. 1990. *J. Geophys. Res.* 95: 9971–81
75. Scotto, J., Cotton, G., Urbach, F., Berger, D., Fears, T. 1988. *Science* 239: 762–64
76. Blumthaler, M., Ambach, W. 1990. *Science* 248: 206–8
77. Roy, C. R., Gies, H. P., Elliott, G. 1990. *Nature* 347: 235–36
78. Brühl, C., Crutzen, P. 1989. *Geophys. Res. Lett.* 16: 703–6
79. Natl. Acad. Sci. 1976. *Halocarbons: Environmental Effects of Chlorofluoromethane Release*. Washington, DC: Comm. Impacts Stratos. Change. 125 pp.
80. Natl. Acad. Sci. 1979. *Protection Against Depletion of Stratospheric Ozone by Chlorofluorocarbons*. Washington, DC: Comm. Impacts Stratos. Change. 392 pp.
81. Natl. Acad. Sci. 1982. *Causes and Effects of Stratospheric Ozone Reduction: An Update*. Washington, DC: Comm. Chem. Phys. Ozone Depletion, Comm. Biol. Effects Increased Solar Ultrav. Radiat. 339 pp.
82. 1990. *Ambio* 19: 279–344

Annual Review of Physical Chemistry
Volume 42, 1991

CONTENTS

(*continued*)